ACCEPTED MANUSCRIPT (STRUCTURES, 2021)

https://doi.org/10.1016/j.istruc.2021.06.072

Geometric design classification of kirigami-inspired metastructures and metamaterials

Yue Sun [a], Wangjie Ye [a], Yao Chen [a,*], Weiying Fan [a], Jian Feng [a], Pooya Sareh [b]

[a] Key Laboratory of Concrete and Prestressed Concrete Structures of Ministry of Education, and National Prestress Engineering Research Center, Southeast University, Nanjing 211189, China
[b] Creative Design Engineering Lab (Cdel), Department of Mechanical, Materials, and Aerospace Engineering, School of Engineering, University of Liverpool, Liverpool L69 3GH, United Kingdom

ARTICLE INFO

Keywords:
Kirigami
Metastructure
Metamaterial
Origami
Pattern
Fractal cut
Lattice

ABSTRACT

In recent years, kirigami – the ancient art of paper-cutting – has been widely studied by scientists and engineers in various fields such as structural mechanics, materials, optics, electronics, robotics, and bioengineering. Kirigami is a combination of slits and creases; therefore, a kirigami structure has a cutting step that is not involved in making an origami structure. In general, a kirigami structure starts from a continuous planar sheet, forms a new shape by cutting or carving, and finally acquires a new structural configuration by stretching, folding, or other external stimuli. Kirigami is considered to be an innovative and effective method for advanced three-dimensional micro- and nano-manufacturing by providing different fabrication strategies through cutting and folding thin sheets. Furthermore, kirigami is generally used as a technique to make (meta)materials and (meta)structures with extraordinary properties such as negative Poisson's ratio. In doing so, a given material/structure is transformed into a metamaterial/metastructure with properties which do not exist in the initial material/structure. In this paper, from the perspective of geometric design, kirigami patterns are categorized into two groups: (1) cut-only kirigami, and (2) cut-and-fold kirigami. Moreover, the patterns are classified into five categories as follows: fractal cut, ribbon, lattice, zigzag, and closed-loop kirigami. Physical models are made and presented to demonstrate the design and geometric properties of these kirigami patterns. Finally, this review summarizes the current developments in kirigami-inspired metastructures and metamaterials and concludes with a future outlook of their potential applications in science and engineering.

1. Introduction

The word 'kirigami' means paper cutting, which is a traditional Chinese and Japanese art with a history of around fifteen centuries [1–11]. In kirigami, a piece of paper is cut, and might be folded, in order to create a new two- or three-dimensional object. In general, a kirigami structure starts from a continuous planar sheet, forms a new shape by cutting or carving, and finally acquires a new structural configuration by stretching, folding, or other external stimuli. In recent decades, kirigami, along with origami (the art of paper folding), have attracted the attention of researchers across science, mathematics, engineering, and architecture [12–60]. Kirigami is generally used as a technique to make (meta)materials and (meta)structures with extraordinary properties such as negative Poisson's ratio. In doing so, a given material/structure is transformed into a metamaterial/metastructure with properties which do not exist in the initial material/structure.

Kirigami metastructures with unique flexibility and stretchability have been used to manufacture macro and micro materials, equipment, structures, and systems [61]. For example, the concept of kirigami graphene was introduced to increase the ductility of graphene [62] and build mechanical metamaterials, which can transform single-layered graphene sheets into deformable parts with microscale dimensions [63]. Thereafter, kirigami has provided a new direction in the research and applications of graphene.

After decades of research and development, 3D microfabrication/nanofabrication is approaching the bottleneck of physical limits. There are two conventional approaches to 3D micro-manufacturing; the first approach includes direct laser writing (LDW) [64] and focused-ion-beam (FIB) [65] techniques that require precise 3D translation [66,67]; and the second approach includes multilayer stacking [68] and

oblique angle deposition [69] that require precise alignment. When the manufacturing precision is within the nanometer range, the above manufacturing methods may become highly costly and time-consuming.

Kirigami is considered as an innovative and effective method for advanced three-dimensional (3D) microfabrication/nanofabrication [70] by providing different manufacturing strategies through cutting and folding thin sheets [71,72]. In general, kirigami patterns are made on a 2D plane, enabling us to flexibly create complex and programmable patterns on the nanometer scale. Subsequently, these 2D structures are folded or bent into 3D configurations [73] by external stimuli. In addition, this method can be applied to a variety of single-layer or multi-layer initial materials, such as metals [74], graphene [63,75] and nanocomposites [76,77]. Compared with traditional 3D printing technologies, 3D manufacturing using kirigami has many advantages, including wider range of applicable materials, higher manufacturing accuracy, and feasibility and manufacturability of more complex patterns.

A kirigami structure has a cutting step which is not involved in making an origami structure. Origami directly transforms uncut paper into an intricate 3D structure by folding along crease lines [78]. There is a wide range of methods to design fold patterns to achieve origami structures, including empirical methods, trial and error processes, and numerical methods based on computational geometry [79,80], geometric-graph-theoretic method [81,82], as well as metaheuristic approaches using genetic algorithm [82] and particle swarm optimization [83]. The empirical method is relatively random, and the numerical method involves a lot of analysis or computational challenges [82].

In comparison with origami methods, which are usually based on a single flat sheet for folding the desired structure, kirigami methods can be based on multiple layers and produce more complex structures. As a result, after cutting the paper appropriately based on kirigami techniques, the folding process could generally be easier to obtain a rich variety of complex metamaterials and metastructures [82–84]. Kirigami structures can be folded and unfolded repeatedly by selecting suitable materials, such as composite materials with a heat [85], humidity [86], electric [87], and light [88] sensitive interlayer.

In this paper, kirigami patterns are categorized into two groups: (a) cut-only kirigami, and (b) cut-and-fold kirigami. Under these two general categories, this review classifies five types of kirigami objects, including fractal-cut kirigami, ribbon kirigami, lattice kirigami, zigzag kirigami and closed-loop kirigami, as illustrated in Fig. 1.

2. Fractal-cut kirigami

Kirigami techniques involving only cutting – called *cut-only* kirigami in this paper – are usually used to make 2D materials and structures with enhanced elasticity. Cut-only kirigami patterns can be divided into two categories; one uses a method known as 'fractal cut' [89] to create rotating units, and the other involves strip-shaped cutting of the paper to form a curved unit. Both types can achieve large strains that cannot be attained by the initial material through external tension or compression. Importantly, the tensile properties of kirigami sheets are largely determined by the specific kirigami patterns rather than the tensile properties of the initial material, leading to the development of metamaterials/metastructures.

Inspired by the hierarchical structure and recursive division of stem cells in nature, Cho et al. [89] demonstrated that the fractal cut method could fit a piece of sheet to a wide range of graphic boundaries,

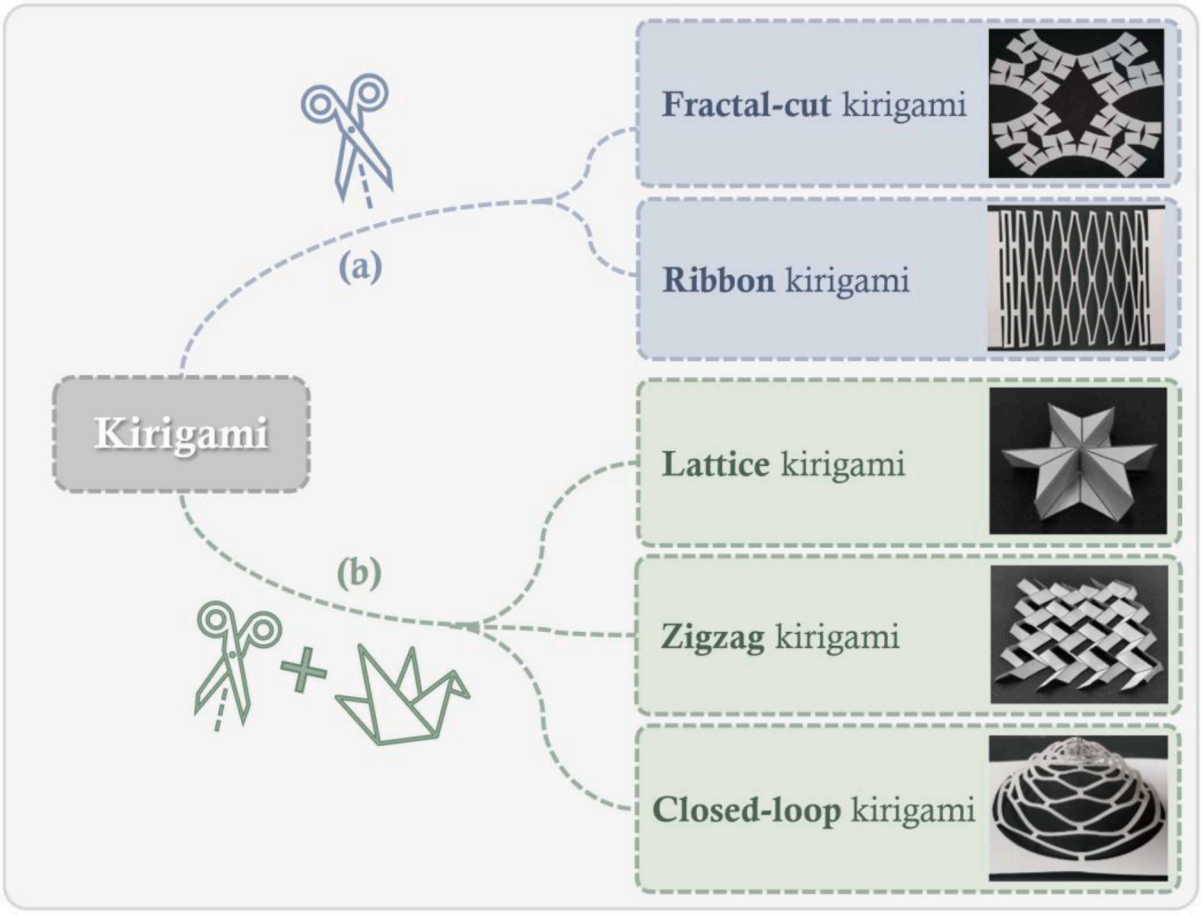

Fig. 1. A general classification of kirigami structures produced by (a) cutting only, and (b) cutting and folding.

including 2D and 3D shapes. The rotating units formed by hierarchical cut patterns are polygons, as illustrated in Fig. 2. For example, a square is hierarchically cut into square rotating units connected by hinges, whereas a hexagon is correspondingly cut into triangles. As a result of its hierarchical formation method, the fractal cut kirigami has remarkable fitting ability and stretchability. Considering the square hierarchical cutting as an example, the maximum theoretical lateral strain of the level-1 and level-2 structures are respectively 43% and 62%. Interestingly, Cho et al. [89] showed experimentally that the square was expanded to 800% of its original area. Based on this research, Tang et al. [90] improved the stretchability and compressibility of such meta-structures by using rectangular units with an aspect ratio of 2:1 which dramatically increases the lateral strain of the level-1 and level-2 structures to 124% and 156%, respectively. A geometric model was proposed to predict the tensile properties and Poisson's ratio of kirigami metamaterials. For the level-1 structures, the nominal strains along the x- and y-directions denoted respectively by ε_x^{Lvl-1} and ε_y^{Lvl-1}, and Poisson's ratio v^{Lvl-1}, can be expressed as

$$\varepsilon_x^{Lvl-1} = cos\left(\frac{\theta}{2}\right) + \frac{1}{m} sin\left(\frac{\theta}{2}\right) - 1 \tag{1}$$

$$\varepsilon_y^{Lvl-1} = cos\left(\frac{\theta}{2}\right) + msin\left(\frac{\theta}{2}\right) - 1 \tag{2}$$

$$v^{Lvl-1} = -\frac{d\varepsilon_x^{Lvl-1}}{d\varepsilon_y^{Lvl-1}} = -\frac{d\varepsilon_x^{Lvl-1}/d\theta}{d\varepsilon_y^{Lvl-1}/d\theta} = \frac{cos(\theta/2)/m - sin(\theta/2)}{mcos(\theta/2) - sin(\theta/2)} \tag{3}$$

where $m = a/b$ is the aspect ratio of the rectangle, where a and b respectively denote width and length. In Eqs. (1)–(3), θ is expansion angle, as illustrated in Fig. 2f-g. It can be concluded from Equation (3) that Poisson's ratio $v^{Lvl-1}$is negative when the tensile strain is small. As the tensile strain gradually increases, v^{Lvl-1} transitions from zero to positive. For the level-2 structure, after the geometric model considers the level-1 cut structure unit as a rectangle, the equation is the same as that of the level-1 structure. It is important to note that the rotation angles θ of the level-1 level-2 structures are independent.

For the shape of the rotating unit, Tang et al. [90] introduced a circular cut in the initial square unit. This method forms hierarchical porous-square-unit metamaterials, which further enhance stretchability. Furthermore, it enables the kirigami sheets to have superior compression performance in comparison with other kirigami patterns. When

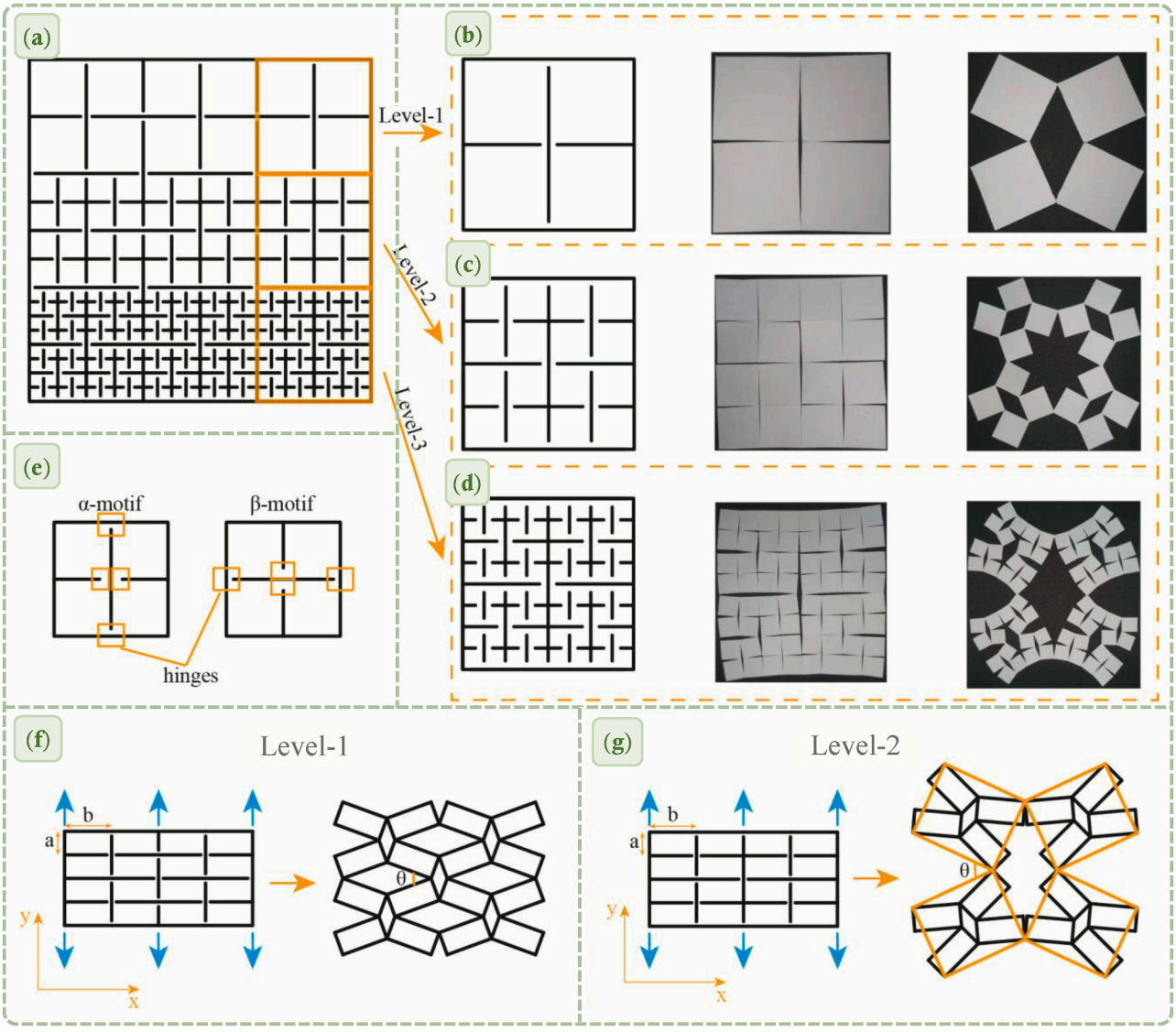

Fig. 2. (a) A fractal cut pattern with square units. (b-d) Square fractal cutting examples of (b) level-1, (c) level-2, and (d) level-3, where the black lines indicate the cut lines. (e) Two level-1 cutting motifs. (f & g) Deformation of (f) level-1, and (g) level-2 rectangular fractal cut kirigami structures after being stretched in the y-direction.

compressed, the pores in the porous-square-unit materials are compressed and closed. Thus, the materials exhibit a macroscopic compression behavior. Moreover, a re-entrant geometry was introduced to replace rigid square rotating units which led to improved stretchability and compressibility.

There are two main cutting methods for hierarchical cutting, namely α-motif and β-motif, as displayed in Fig. 2. Alternating cutting motifs will have greater maximum lateral strain than a single-motif cut pattern. In each cutting level, using the same cutting method can facilitate regular stretch deformation, whereas to fit arbitrary and complex boundary conditions, inhomogeneous deformation is required, which can be achieved by either mixing α-motif and β-motif at the same level, or designing distinct numbers of cutting levels in different areas [89]. An et al. [91] achieved programmable information encryption by combining different hierarchical kirigami patterns, where one kirigami pattern composes information, and another pattern fills the vacant part. Jin et al. [92] combined a kirigami sheet and an elastic membrane, and utilized the kirigami sheet to control the deformation of the elastic membrane when it was inflated. By programming the geometric parameters of the kirigami pattern, the kirigami balloon can simulate various geometries with circular cross-sections (e.g., vases, fish hooks, and pumpkins) after being inflated.

The stretching of hierarchical cut structures is based on the free rotation of their constituting rotating unit. However, the hinges connecting the rotating units in actual materials may fail due to stress concentration or large deformations. Elastic materials can resist tear to a certain extent, but when hierarchical kirigami pattern is applied to other materials (e.g., brittle materials), the problem of hinge failure cannot be avoided. Tang et al. [93] first studied the mechanical properties of hierarchical cut structures under the real properties of the initial material. Based on numerical simulations and experiments, the hinge of hierarchical cut structures was optimized to the dog-bone-like shape. In addition, they proposed that the width of the hinge should vary with the change of level. The hinge width of level-1 should be the largest, while the hinge width of the smallest sub-unit should be the smallest. Because the hinge with the smallest width is more susceptible to deformation when stretched and has the largest number, it can absorb more energy for the level-1 hinge and reduce the opening angle of the level-1 hinge [93]. In addition, creases have been introduced to the design of the hinges. Three creases are added to the vertices of the cut lines. Consequently, the hinge at the vertex will be folded along the crease lines when the rotating unit rotates [94]. This strategy can avoid stress concentration and therefore tearing at the hinges.

Babaee et al. [95] took inspiration from the claws and scales of creatures and designed a kirigami pattern resembling fish scales. Taking this kirigami pattern as an example, Rafsanjani et al. [96] verified that the kirigami shell exhibit discontinuous phase transitions during stretching through theoretical analysis, numerical simulation, and experiments. It should be noted that only the buckled phase exists in the kirigami sheet with zero curvature, whereas the buckled and unbuckled phases can coexist in the cylindrical kirigami shell with non-zero curvature. Changing the geometric characteristics of the kirigami pattern and the curvature of the kirigami shell can change the position, sequence, and recognition of the discontinuous phase transition. Based on this property, the movable surface of linear actuators can be designed.

Fractal-cut kirigami is capable of creating flexible shapes; consequently, many studies have been conducted on shape fitting and hinge optimization for such structures. Furthermore, there have been a few studies on the practical applications of fractal-cut kirigami which mainly focused on shape fitting [89] and soft robotics [97]. However, research on the control of the rotational angle in fractal-cut kirigami has been limited.

3. Ribbon kirigami

Another cut-only kirigami pattern is the ribbon pattern, which was originally proposed to improve the ductility of graphene. Qi et al. [62] divided the tension process of graphene kirigami into four stages, while the tensile load is applied perpendicular to the length of the ribbon. Firstly, when the tensile deformation is small, the ribbon rotates around the hinge to produce out-of-plane distortion. At this stage, the material itself is not stretched and thus no stress is induced. Secondly, the tensile deformation increases, and the deformation of the material contributes to the total deformation. The stress of the ribbon increases, and the material stress and strain at the hinge is the largest. Thirdly, the tensile deformation further increases, and the kirigami structure yields due to stress concentration at the hinges. Finally, the kirigami structure is damaged by the tearing of the hinges. The whole process is shown in Fig. 3a-d. Whether the initial material is elastic or plastic, the deformation process of the kirigami structure after being stretched remains qualitatively similar.

The strain capacity of the kirigami structure is mainly concentrated in the second stage of deformation [98]. Moreover, the second stage is in a state of elastic deformation with little loss of strain energy. Han et al. [99] introduced the beam deflection theory to study the tensile response of kirigami metallic glass in the elastic phase. The combination of two beam elements replaced one side of the diamond pattern produced by stretching. A prediction model that can calculate the critical force of the first and second stages was proposed. There are some studies on plastic strain in the third stage and fracture in the fourth stage. A recent study found that, the larger the size of the kirigami pattern unit, the greater the fracture force required to tear the kirigami structure [99]. When the kirigami structure is stretched, the deformations of the two ends and the middle part of the structure are different. Because the end regions are close to the tensioned position, deformation is limited. In order to better simulate the actual situation of stress–strain behavior and potential fracture, a series spring model was proposed [100]. Springs with certain stiffness characteristics were used to simulate different deformation areas, and each cycle was regarded as one spring.

Scientists have carried out various studies on the shapes [98,101], cut-distances [77,101,102], and hinge forms [98] of kirigami patterns to increase the tensile strain of kirigami structures. Experimental studies [98] show that the kirigami structures produced by straight-cutting and curve-cutting have similar stretchability, where the limit of tensile strain of the curve-cut kirigami slightly increases. For instance, a straight-cut pattern is depicted in Fig. 3e, while a curve-cut pattern is shown in Fig. 3f. The geometric parameters that affect the critical buckling load and stretchability of the kirigami structure mainly include the horizontal distance, vertical distance, and length of the slits. In general, the thinner the ribbon formed by cutting, the better the stretchability and the larger the size at the hinge, the greater the critical buckling load. The experimental and numerical results of Shyu et al. [77] showed that the increase of the horizontal (or vertical) distance and the decrease of slit length improve the critical buckling load. They reported that the increase of horizontal distance and slit length and the decrease of vertical distance enhance the stretchability. Isobe et al. [102] proposed a theoretical explanation to qualitatively verify this conclusion. For the hinge design, Chen et al. [98] designed circular cuts at both ends of the slit, as shown in Fig. 3i-j, and compared the influence of the radius on the strain energy loss. Due to the existence of the circular gap, the plastic deformation of the material at the hinge is small during stretching. As a result, the strain energy loss is proportional to the radius of the circle. Similarly, Hwang et al. [103] added orthogonal small incisions at both ends of the slit, increasing the ultimate tensile strain to twice and the elasticity by 30 times.

When the ribbon kirigami structure is stretched, the ribbon will bend upward or downward, and its deformation mode is not unique. This bistable deformation mode will cause great difficulties in the application of ribbon kirigami structures. In order to control the deformation mode

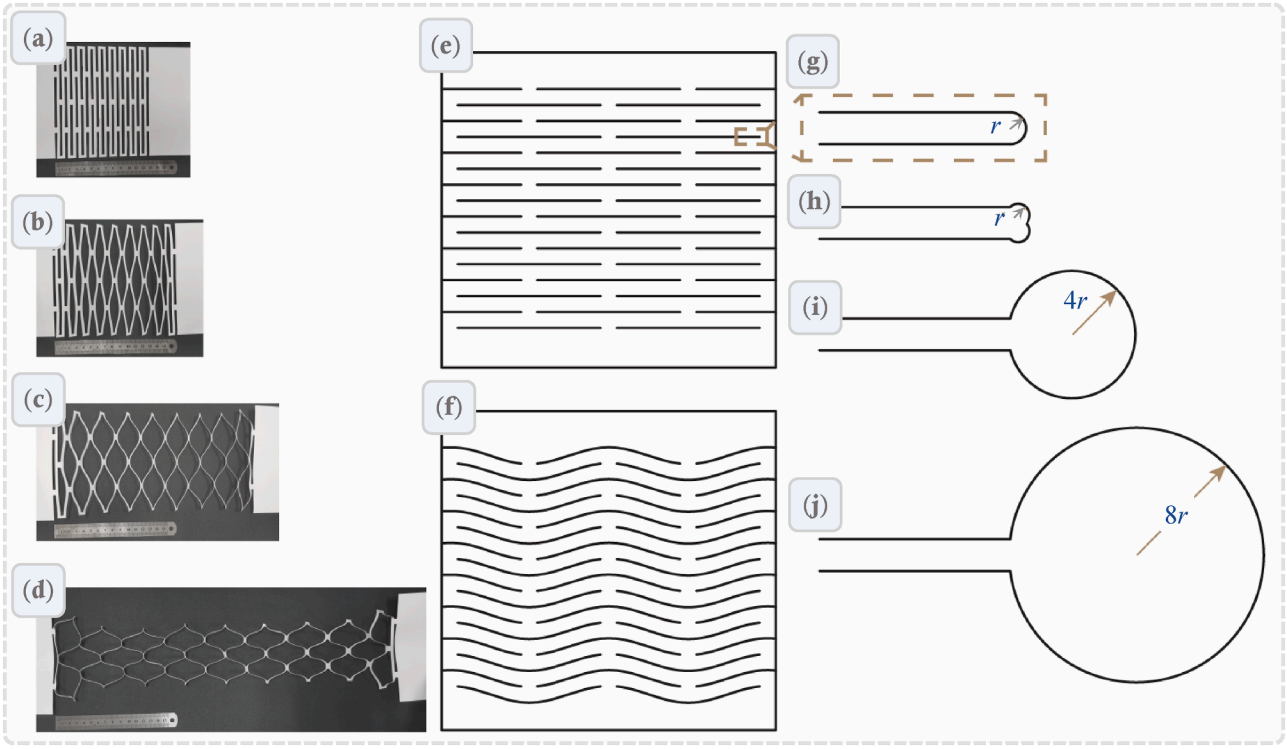

Fig. 3. Ribbon kirigami. Parts (a)-(d) show the stretching process of ribbon kirigami. (e) Straight-cutting. (f) Curve-cutting. Figures (g)-(j) show four types of hinges, including (g) ordinary U-shaped cut hinges, (h) dog-bone-like cut hinges, (i) 4*r* circular hinges, and (j) 8*r* circular hinges.

during stretching and realize the programmability of kirigami structures, some research work has been performed. Tang et al. [104] proposed a kiri-kirigami method that introduces shallow grooves on the front or back of the hinges. The deformation of the kirigami structure when stretched will be affected and induced by defects (grooves). Ribbons tend to close the grooves and twist around them, thus achieving the predetermined deflection. Yang et al. [105] analyzed the occurrence of symmetric bending (bistable unit cell) and antisymmetric bending (monostable unit cell) from the perspective of energy. Both the theory of minimum energetic state and experimental results showed that antisymmetric bending is in a lower energy state. Switching between different bending modes requires a certain amount of bending energy. They adjusted the geometric parameters of the kirigami pattern to achieve different bending modes under the same stretching force.

The ribbon kirigami structure can greatly improve the elasticity of the material with a simple manufacturing process. Therefore, it has a wide range of applications for various materials and structures. The ribbon kirigami was first applied to graphene materials [63,75,106]. In recent years, it has been gradually applied to other materials such as metallic glasses [99,101], shape memory alloys [107], monolayer MoS_2 [108], MnO_2 nanowire composites [76], and carbon nanotubes [109]. The ribbon kirigami structures have been widely exploited in the design and fabrication of energy and biomedical devices.

4. Lattice kirigami

Kirigami design involving cutting and folding is an emerging approach to 3D nanomanufacturing. Folding is the key to the conversion of 2D sheets to 3D structures. Such a kirigami structure is cut off appropriate parts, and then folded to close the missing part to form a 3D structure.

Inspired by phyllotaxis [110,111], Castle et al. [112] proposed the concept of lattice kirigami. Notably, lattice kirigami is based on the Bravais lattices. They introduce defects into the sheets, including cutting and removing (or adding) wedges [113], and then perform dislocations or disclinations to form 3D structures. There are five types of 2D Bravais lattices, among which triangle lattices and square lattices are suitable for kirigami structures [113].

Current research on lattice kirigami mainly focuses on the honeycomb (triangular) lattice [112,114]. Castle et al. [112] removed some wedges from the hexagonal lattice to form a 5–7 dislocation pair and a 2–4 dislocation pair, which are illustrated in Fig. 4a-b. The wedge vertex removed by a 5–7 dislocation pair is located at the center of the hexagon, and the vertex angle is $\pi/3$. The wedge vertex removed by a 2–4 dislocation pair is located at the center of the hexagon, and the vertex angle is $2\pi/3$. The heights of the steps formed by folded 5–7 and 2–4 dislocation pairs are different. The height of a 5–7 dislocation pair is $\sqrt{3}$ times the side length of the hexagon, and the height of a 2–4 dislocation pair equals the side length of the hexagon. The height difference between them indicates that they cannot exist simultaneously around a plateau [112]. Both 5–7 and 2–4 dislocation pairs are bistable and can be folded up or down, which is important to achieve programmable kirigami. In addition, Castle et al. [112] proposed the concepts of climb cut and glide cut, as shown in Fig. 4c-d. The kirigami patterns illustrated in these figures are all formed by the 5–7 dislocation pairs.

Subsequently, based on the bistable behavior of the 2–4 dislocation pairs, Sussman et al. [114] proposed a multifunctional lattice kirigami. The smallest unit is composed of six hexagons surrounding an excised hexagon, as shown in Fig. 4e. Folded along the parallel mountain and valley creases, the excised hexagon can be closed, and the triangular platform formed by the creases will be at different height platforms. A unit cell can form two modes by adjusting the mountain and valley creases, two-level platform, and three-level platform. Even so, the involved folding allows the height difference between the adjacent platforms to be one grid. The drop of the two levels platform appears on the opposite triangular platform. The height difference of each level of the platform is $1/\sqrt{3}$ times the side length of the platform triangle. The unit cells are arranged periodically according to the lattice vector, and the surface of any curvature can be fitted. The range of gradients that can be fitted depends on the ratio of height to platform width [114]. The

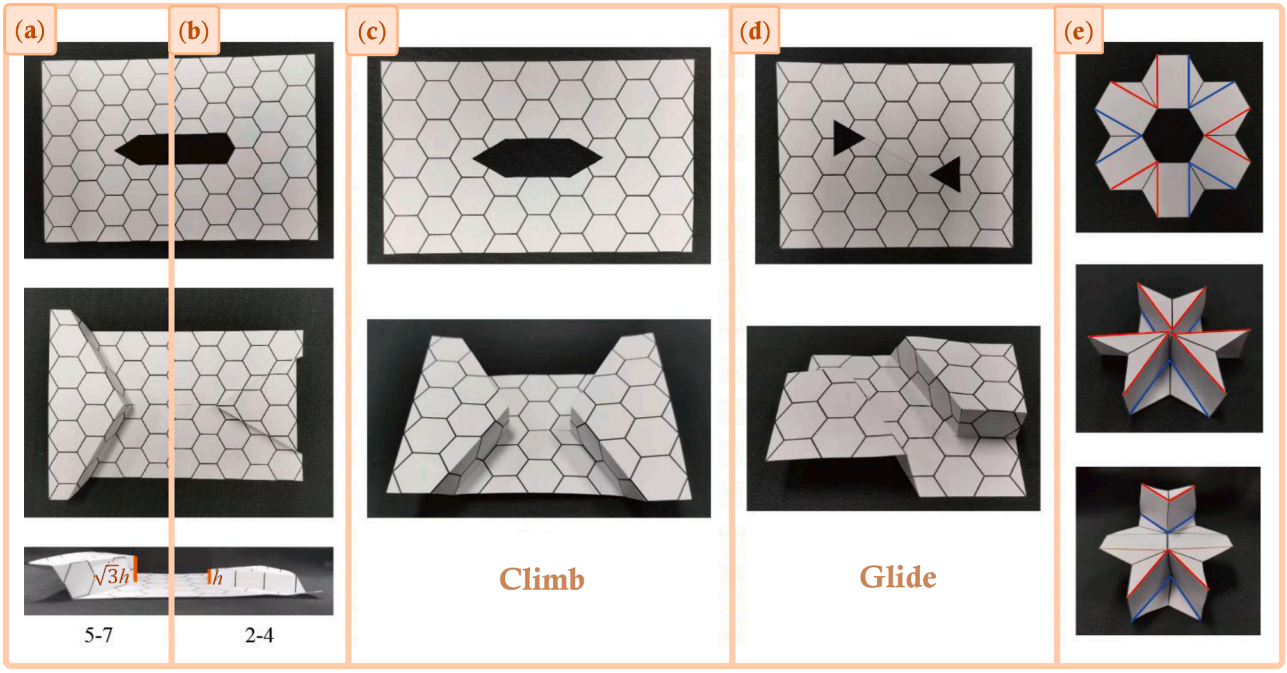

Fig. 4. Lattice kirigami. Two ways to remove the wedge block: (a) a 5–7 dislocation pair, and (b) a 2–4 dislocation pair. (c) Pure climb cut: the gap is closed by folding, and there is no relative sliding between the slits. (d) Pure glide cut: the gap is closed by folding and relative sliding between slits. (e) "Sixon": Six hexagons surround a cut hexagon. Upward or downward steps are formed by folding along the mountain (red) or valley (blue) creases. (For interpretation of the references to colour in this figure legend, the reader is referred to the web version of this article.)

5–7 dislocation pairs also have a similar unit design [114]. However, it needs to be excised in different positions to be folded upward and downward. Fitting different macroscopic curvatures requires completely different designs, thus it is difficult to achieve actual application requirements.

Castle et al. [113] cut a zigzag along the triangular Bravais lattice, then staggered the formed serrations and inserted them. This method creates wrinkles in the paper, similar to the"z-plasty" techniques of plastic surgery [115]. This kind of cutting does not remove parts, and can be called area-preserving lattice kirigami. The zigzag cut essentially forms a pair of Gaussian curvature dipoles and then separates them. With appropriate mountain and valley creases, the Gaussian curvature of the vertex can be changed. The area-preserving lattice kirigami can be carried out continuously, or it can be folded separately and combined with other types of lattice kirigami.

The kirigami patterns of the above lattice kirigami are all based on the triangular/hexagonal Bravais lattice. Since the square Bravais lattice has the same side length and C_{4v} symmetry [116,117], the above lattice kirigami patterns are applicable with slight changes. In addition, Castle et al. [113] explored the lattice unit, which is the basis of the lattice kirigami. According to the rectangular and centered rectangular Bravais lattices with unequal sides, after excising a wedge with an apex angle less than π, the two sides of the apex angle cannot completely overlap due to the unequal length. The last type of Bravais lattice, the oblique lattice, has the potential for lattice kirigami when the four sides are equal (rhombus lattice). The side lengths of the rhombic lattice are equal. However, the angle is still a variable, and it is worth being investigated. Furthermore, the triangular and square lattices are combined into a new lattice according to certain rules. The new lattice should have the same side length and higher symmetry so that the cuts can completely overlap after excising the wedge. The triangular and square lattices form a new lattice around a vertex in the order of STSTT (square-triangular-square-triangular-triangular), which is presented in Fig. 5a [113]. Excise C_{4v} symmetric four-pointed stars from the STSTT tile. Excise C_{4v} symmetric squares (see Fig. 5b) or four-pointed stars (including a square and four triangular lattices) (see Fig. 5c) from the STSTT tile, and the remaining patterns can be folded into 3D structures [113].

Moreover, lattice kirigami with different folding modes under the same lattice can be interlocked at the edges in complementary

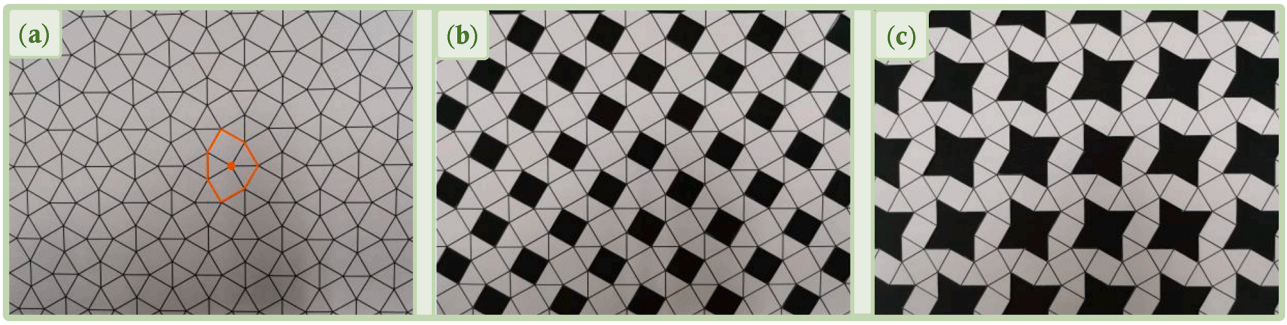

Fig. 5. STSTT tiling. (a) STSTT tiling diagram. (b) A pre-fold pattern formed by removing every other square. (c) Another pre-fold pattern formed by removing four-pointed stars.

polyhedral shapes. Recall that lattice kirigami is useful for fitting various Gaussian curvature surfaces. The basic lattice of lattice kirigami should be further studied.

5. Zigzag kirigami

The folding pattern of the zigzag kirigami is inspired by a classic origami pattern called the Miura-ori which has the desirable characteristics of negative Poisson's ratio [118] and rigid folding [119]. Inspired by the Miura-ori, Eidini et al. [120] combined two single-degree-of-freedom (DOF) zigzag strips with the same kinematics and different unit scales, and proposed a new kirigami metamaterial. Each unit cell of the zigzag strip has a hole, and a large-scale Miura strip corresponds to an n-folded small-scale Miura strip. Therefore, this zigzag kirigami unit cell is called the BCH_n (Basic unit Cell with Hole) unit cell. The mechanical properties of the zigzag kirigami were studied, including the in-plane Poisson's ratio and out-of-plane bending and twisting behavior [120]. The parameter representation of the BCH_n unit cell is shown in Fig. 6a. For the zigzag kirigami with $n = 2$, the in-plane Poisson's ratio of the approximately infinite BCH_2 is expressed as [120]

$$\nu_\infty = -tan^2\phi \frac{4\lambda cos\alpha - cos^2\phi}{4\lambda cos\alpha + cos^2\phi} \tag{4}$$

where $\lambda = a/b$, and ϕ is the angle in the xy plane between edge b and the $\times$ axis [120]. The sign of Poisson's ratio depends on the sign of the numerator in the equation.

Furthermore, Eidini [121] proposed a misplaced zigzag strip kirigami based on the Miura-ori. The misplaced zigzag strip unit cell is shown in Fig. 5b. There are two ways of dislocation of zigzag strips. One is that two sets of adjacent zigzag strips are misaligned upward and downward respectively, and the kirigami structure formed is shown in Fig. 5d. The other is that adjacent zigzag strips are misaligned in the same direction, and the kirigami structure formed is displayed in Fig. 5c. In addition, the geometric parameter [121] changes of the parallelogram voids formed by the dislocation also affect the pattern and folding of the zigzag kirigami, as shown in Fig. 5e. The in-plane Poisson's ratio

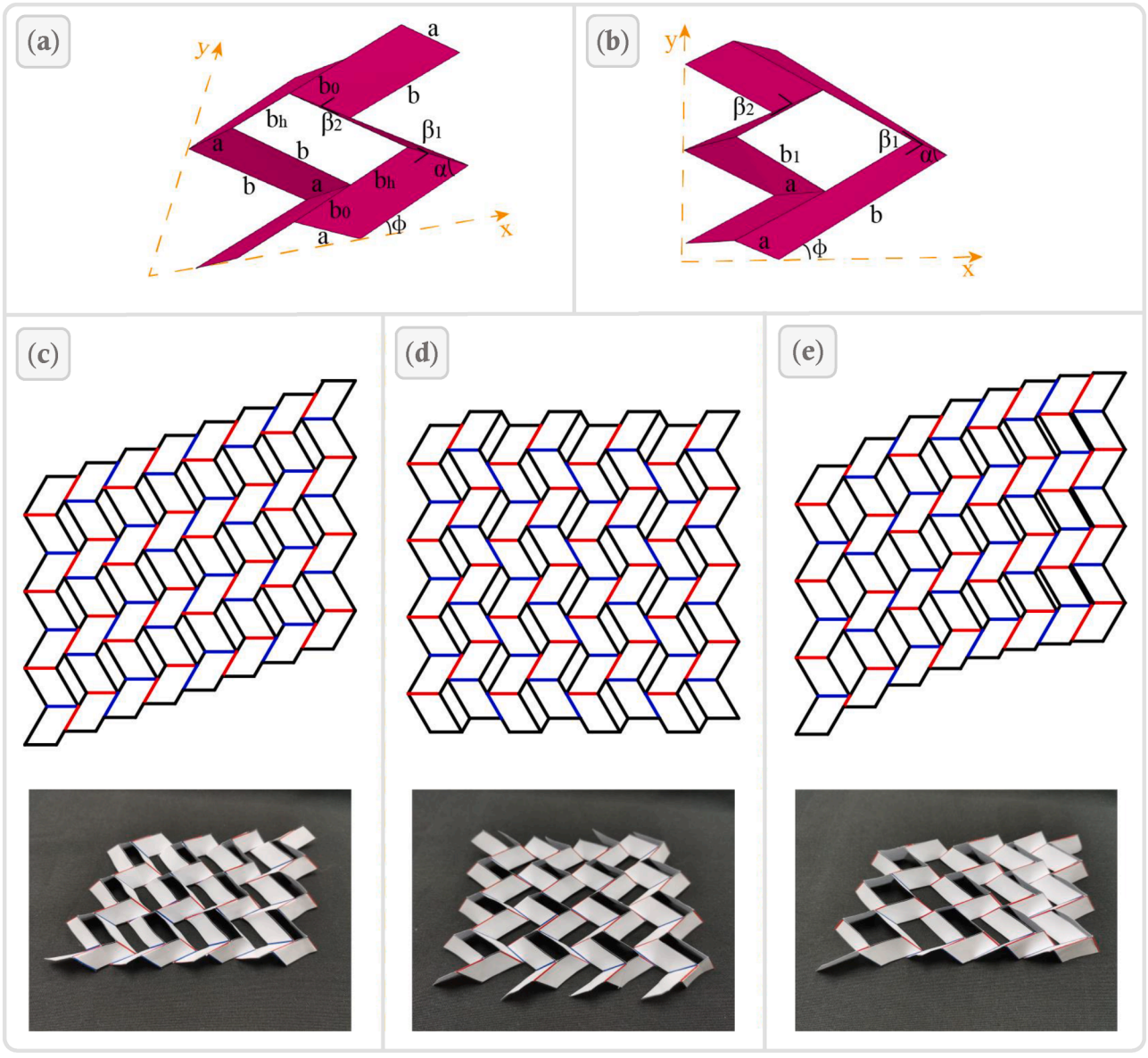

Fig. 6. Zigzag kirigami. (a) Geometry of the ZCH pattern unit cell. (b) Geometry of the BCH_2 pattern unit cell. Adjacent zigzag bars are misaligned in the same direction to form (c), and the two sets of adjacent zigzag bars are respectively displaced upward and downward to form (d). The distance of dislocation is changed to form (e).

of the approximately infinite ZCH (Zigzag unit Cell with Hole) is expressed as [121]

$$\nu_{\infty} = -tan^2\phi \frac{acos\alpha - b_h cos^2\phi}{acos\alpha + b_h cos^2\phi} \quad (5)$$

Similarly, the sign of Poisson's ratio depends on the sign of the numerator.

The ZCH kirigami retains the characteristics of the Miura-ori, including negative Poisson's ratio, stackability, and rigid folding. Due to the existence of the holes, the zigzag kirigami has lower density and higher programmability. These characteristics make it have a wider application prospect than the Miura-ori.

6. Closed-loop kirigami

On the nano scale, kirigami methods can break through the limitations of micro-3D manufacturing, and induce folding, bending, and twisting through cutting and external stimuli. In 2018, Liu et al. [74] proposed a kirigami-inspired nano pinwheel-like pattern with large optical chirality. This nano-kirigami first cuts four rotationally symmetric slits on the 2D gold film sheet, as shown in Fig. 7. Then, the gold film is irradiated by a global programmable ion beam. The sputtering of gold atoms and the implantation of gallium atoms on the gold film make the gold film subject to tensile stress and compressive stress, respectively. The tensile and compressive stresses along the thickness direction of the gold film make the gold film bend towards the irradiation direction (see Fig. 7b). The nano pinwheel-like pattern irradiated by the global focus ion beam (FIB) [122-124] will be convex and twisted under the equilibrium of stress. Tang et al. [125] studied the optical properties of this symmetric nano-kirigami pattern and found that it has giant nonlinear optical circular dichroism. Liu et al. [126] explored the optical properties of the C_3, C_4, and C_6 symmetric kirigami patterns.

Li and Liu [127] named the above-mentioned type of FIB-based nano-kirigami *closed-loop* nano-kirigami. The kirigami characteristic of this closed-loop system is that the parts in a closed-loop will influence and restrain each other when folded/bent/twisted. The deformation of the closed-loop kirigami after ion beam irradiation is not only affected by a single crease, but is also dependent on the geometric topology and stress equilibrium of the entire close-loop system. Therefore, the deformation process and results of closed-loop nano-kirigami patterns are difficult to predict. Liu et al. [74] proposed a comprehensive mechanical model to build an accurate nano-kirigami model, and proved that this model can predict the deformed structure well through experiments and numerical simulations. It has a similar topology with pinwheel-like patterns, including combined multiple Fibonacci spirals (see Fig. 7c) and concentric arc structure (see Fig. 7a).

The boundary conditions, width, radian inside the closed-loop kirigami pattern and ion beam dosage will affect the formed 3D structure. Therefore, the closed-loop kirigami has considerable potential for programmability. In addition, compared with other FIB-based nano-manufacturing methods [128,129], the closed-loop kirigami has simpler steps and higher precision. The closed-loop nano-kirigami has potential for applications in optical/mechanical devices and electromagnetic components.

7. Discussion and conclusions

This paper reviewed the research progress of kirigami-inspired metastructures and metamaterials from the perspective of geometric design. We summarized the latest developments in the field of kirigami according to five types of kirigami patterns. For the fractal-cut kirigami, the ductility of square cutting, porous square cutting, two fractal cutting methods, hinge design, and the discontinuous phase transition of the kirigami shell were discussed. For the ribbon kirigami, the stretching process of kirigami metamaterials was introduced, and the shape of the tape-shaped pattern, cutting distance, and hinge form were investigated. For the lattice kirigami, the design principle and the method to fit Gaussian surface were discussed. The properties of zigzag kirigami are partially similar to the Miura-ori. For the closed-loop kirigami, the deformation and optical characteristics were reviewed. A classification

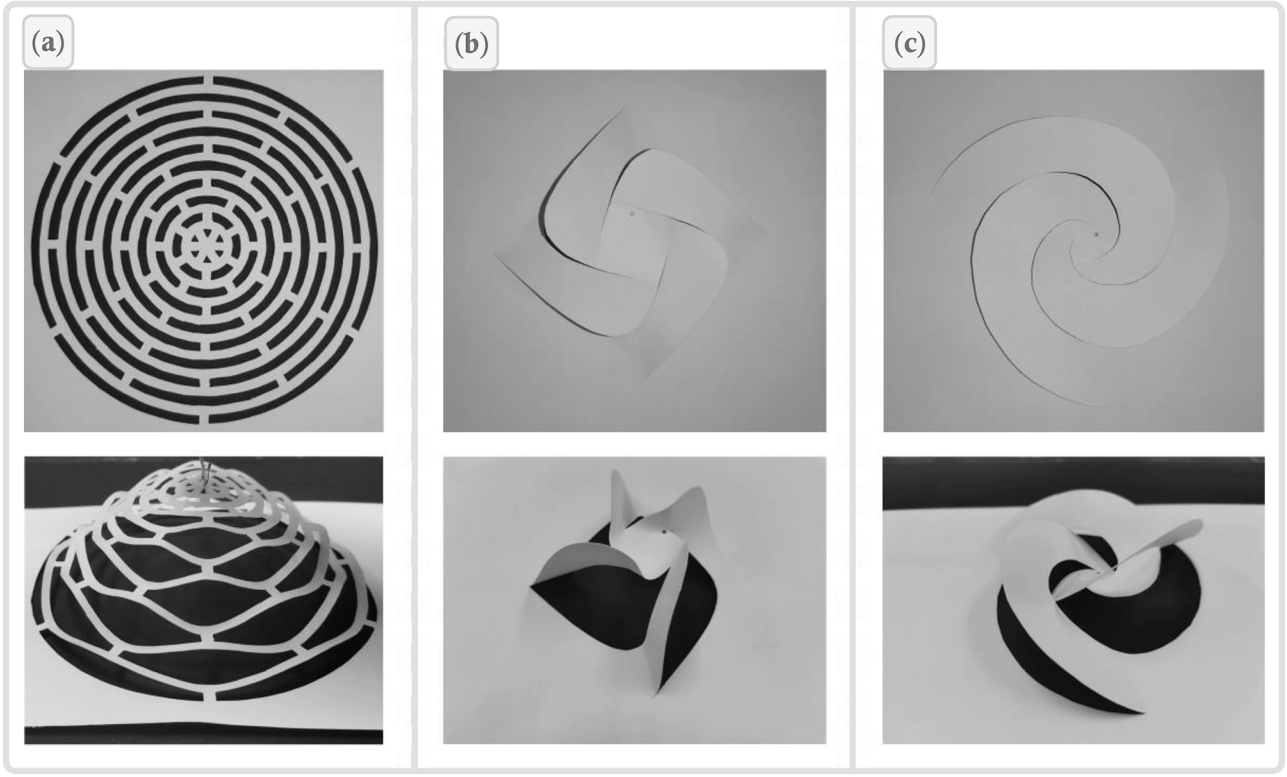

Fig. 7. Closed-loop kirigami: (a) Concentric arc structure. (b) C_4 symmetric pinwheel-like structure. (c) Combined multiple Fibonacci spirals structure.

of these kirigami patterns was presented.

The metastructures and metamaterials inspired by kirigami have many outstanding properties. For example, the cut-only kirigami has excellent ductility. The square fractal-cut kirigami sheets can be extended to 800% of its original area [90], and the ribbon kirigami can be stretched to 30 times its original length [103]. The fractal-cut and lattice kirigami can fit Gaussian surfaces with a certain range of curvatures [89,114]. This plays a major role in fitting a curved surface with a plane. The zigzag kirigami has special mechanical properties such as negative Poisson's ratio [120,121]. Meanwhile, it has a much smaller density and programmable characteristics, compared with the Miura-ori. Some forms of closed-loop kirigami structures have important applications in the field of nano optics.

Therefore, kirigami has a wide range of applications in the fields of solar energy, optics, electricity, magnetism, metamaterials, and biomedicine. Inspired by the orthogonal fractal-cut kirigami, Sedal et al. [97] used a kirigami structure to make soft deployable crawling robots. The flexibility of the geometric parameters of the kirigami structure is conducive to the realization of the programmable stiffness and kinematics of soft robots. Moreover, the ribbon kirigami structure is widely used in the fields of energy and medical equipment due to its huge ductility. A supercapacitor [76] with a customizable shape with a tensile strain of up to 500% was proposed in 2017. This supercapacitor can be made into an energy storage device with artistic appearance and retractable performance, and also has stable sensing performance when worn on the arm. Similarly, Song et al. [130] proposed stretchable lithium-ion batteries based on kirigami, which can stably power smart watches in experiments. Lamoureux et al. [131] used ribbon kirigami for the study of dynamic solar tracking. The angle and orientation of the strip slope can be realized by adjusting the displacement and height of both ends of the strip-shaped cut structure. The solar tracking device designed based on the kirigami design principle is lighter and more economical than traditional devices. Wu et al. [132] proposed triboelectric nanogenerators based on a kirigami structure which can obtain energy through various sports. Dijvejin et al. [133] designed a wireless sensor by mixing two sizes of ribbon kirigami structures, combined with split-ring resonators. In the area of medical technologies, kirigami structures are mainly used in wearable health monitoring devices. Yamamoto et al. [134] designed a printed combined health monitoring device. It can adhere to the skin to monitor body temperature, electrocardiogram, and exercise status. Jang et al. [135] and Guo et al. [136] respectively proposed wearable heating devices based on different conductive papers and kirigami structures. The pinwheel-like closed-loop kirigami has massive nonlinear optical circular dichroism [74,125] which is of great significance in nano-scale optical research.

The current research on kirigami structures mainly focuses on theoretical and applied conceptual design. Very few kirigami studies are actually applied to the development of practical equipment. Kirigami structures are mainly utilized as a structural skeleton or carrier in various optical, electrical, and medical devices. There are many other potential research opportunities on kirigami from theory to practical applications.

When using real materials to fold, the thickness of the materials should be considered. In recent years, there have been many studies on self-folding and stretching on macro and micro scales. However, whether it can stably maintain the folded state, or fold/unfold as required, still needs to be studied. In addition, kirigami-inspired metastructures and metamaterials are usually programmable due to the rich diversity of cutting patterns and folding methods. Some of these have already been applied successfully, such as inflatables [92] with programmable shapes inspired by the square fractal cutting, tracking solar cells [131] inspired by the ribbon kirigami, and optical chiral materials [126]. Although there are a few related studies, there is still a lack of systematic research on the programmable characteristics of kirigami. At present, most of the designs of kirigami patterns are inspired by experience or practice, whereas for origami crease pattern design, there are established mathematical and geometric methods available. Based on geometric topology and analysis, we need to further analyze and design kirigami methods to create and optimize novel kirigami patterns with desirable properties. In addition, while theoretical work on some kirigami patterns is almost mature, research on their engineering applications is rarely carried out. The properties of chosen materials, manufacturing methods, equipment, and product performance tests need to be carried out. Kirigami is still a nascent research field, so it is believed that it will have further developments in the future.

Declaration of Competing Interest

The authors declare that they have no known competing financial interests or personal relationships that could have appeared to influence the work reported in this paper.

Acknowledgements

This work was supported by the National Natural Science Foundation of China (Grants No. 51978150 and 5205041033), the Southeast University "Zhongying Young Scholars" project, and the Fundamental Research Funds for the Central Universities. The corresponding author would like to acknowledge financial support from the Alexander von Humboldt-Foundation for his academic research at Max-Planck-Institut für Eisenforschung GmbH. The authors are grateful to the anonymous reviewers for their valuable comments.

References

[1] Bangay S. From virtual to physical reality with paper folding. Comput Geom Theory Appl 2000;15(1):161–74.
[2] Bodolec C. The Chinese paper-cut: from local inventories to the unesco representative list of the intangible cultural heritage of humanity. Heritage Regimes State 2012:249.
[3] Cranston EA, Cranston FE. Gifts from the hyde collection of Japanese books and manuscripts. Annual Report Fogg Art Museum 1974:38–47.
[4] Fairchild CA. Kirigami: The art of 3-dimensional paper cutting (book review). Library J 2000;125(11):78.
[5] Li Y, Yu J, Ma K, et al. 3D paper-cut modeling and animation. Comput Anim Virtual Worlds 2007;18(4–5):395–403.
[6] Moor I. The ambrotype—research into its restoration and conservation—part 1. Paper Conserv 1976;1(1):22–5.
[7] Stalker NK. Prophet motive: Deguchi Onisaburô and the transformation of religion in modern Japan. Stanford University, 2002.
[8] Wang W. Guangling paper-cut and Japanese paper-cut. J Shanxi Datong Univ Soc Sci 2012;26(02):110–2.
[9] Wang X. Lucky motifs in Chinese folk art: Interpreting paper-cut from Chinese Shaanxi. Asian Stud I 2013;1(2):123–41.
[10] Wang Z, Xiao H, Lu Y. The intellectual property protection of paper-cut art in China. J East China Jiaotong Univ 2008;25(05):122–6.
[11] Yang CHS. Cross-cultural experiences through an exhibition in China and Switzerland: "The art of paper-cutting: East meets West". Notes History Art 2012;31(3):29–35.
[12] Ahn BY, Shoji D, Hansen CJ, et al. Printed origami structures. Adv Mater 2010;22(20):2251–4.
[13] Auckly D, Cleveland J. Totally real origami and impossible paper folding. Am Math Monthly 1995;102(3):215–26.
[14] Barreto PT. Lines meeting on a surface. The "Mars" Paperfolding 1997.
[15] Beatty RD, Yamaguchi Y. Origami: From Japanese folk art to American popular art. J Popular Cult 1976;9(4):808.
[16] Bern M, Hayes B. The complexity of flat origami. SODA 1996;96:175–83.
[17] Cowan B, von Lockette PR. Fabrication, characterization, and heuristic trade space exploration of magnetically actuated Miura-ori origami structures. Smart Mater Struct 2017;26(4):45015.
[18] Demaine ED, Demaine ML, Mitchell JS. Folding flat silhouettes and wrapping polyhedral packages: New results in computational origami. Comput Geometry 2000;16(1):3–21.
[19] Demaine ED, O'Rourke J. Geometric folding algorithms: linkages, origami, polyhedra. Cambridge University Press, 2007.
[20] Douglas SM, Marblestone AH, Teerapittayanon S, et al. Rapid prototyping of 3D DNA-origami shapes with caDNAno. Nucl Acids Res 2009;37(15):5001–6.
[21] Dureisseix D. An overview of mechanisms and patterns with origami. Int J Space Struct 2012;27(1):1–14.
[22] Geretschläger R. Euclidean constructions and the geometry of origami. Math Mag 1995;68(5):357–71.
[23] Holland GE, Trevallyn-Jones M. The structural behaviour of concrete origami building panels. Archit Sci Rev 1984;27(4):98–101.

[24] Horner G, Elliott M. A fabrication and deployment approach for a Miura-ori solar sail model. 2002.
[25] Huang A. Computational origami: the folding of circuits and systems. 1992, 31 (26): 5419–5422.
[26] Hull T. Planar graphs and modular origami, 1994.
[27] Hull TC. Origami design secrets: Mathematical methods for an ancient art. Math Intell 2005;27(2):92–5.
[28] Hunt GW, Ario I. Twist buckling and the foldable cylinder: an exercise in origami. Int J Non Linear Mech 2005;40(6):833–43.
[29] Huzita H. Axiomatic development of origami geometry, 1989.
[30] Kanade T. A theory of Origami world. Artif Intell 1980;13(3):279–311.
[31] Kato J, Watanabe T, Nakayama T, et al. A model-based approach for recognizing folding process of origami. IEEE 1998.
[32] Kidambi N, Wang KW. Dynamics of Kresling origami deployment. Phys Rev E 2020;101(6–1):63003.
[33] Kresling B, Abel JF, Natural twist buckling in shells: from the hawkmoth's bellows to the deployable Kresling-pattern and cylindrical Miura-ori. Proceedings of the 6th International Conference on Computation of Shell and Spatial Structures. 2008, 11: 12–32.
[34] Kuzyk A, Laitinen KT, Törmä P. DNA origami as a nanoscale template for protein assembly. Nanotechnology 2009;20(23):235305.
[35] Lang RJ. Origami: Complexity increasing. Eng Sci 1989;52(2):16–23.
[36] Lang RJ. The science of origami. Phys World 2007;20(2):30–1.
[37] Liu J, Ou H, Zeng R, et al. Fabrication, dynamic properties and multi-objective optimization of a metal origami tube with Miura sheets. Thin Wall Struct 2019; 144:106352.
[38] Miura K. Method of packaging and deployment of large membranes in space. Inst Space Astronaut Sci Rep 1985;618:1–9.
[39] Miura K. Triangles and quadrangles in space. Editorial Universitat Politècnica de València 2009.
[40] Miura K, Natori M. 2-D array experiment on board a space flyer unit. Space Solar Power Review 1985;5(4):345–56.
[41] Nangreave J, Han D, Liu Y, et al. DNA origami: A history and current perspective. Curr Opin Chem Biol 2010;14(5):608–15.
[42] Nojima T. Modelling of folding patterns in flat membranes and cylinders by origami. JSME Int J, Ser C 2002;45(1):364–70.
[43] Nojima T. Origami modeling of functional structures based on organic patterns. Kyoto University, 2002.
[44] Pedersen JJ. N-gami, a variation of origami. Math Teacher 1976;69(1):34–8.
[45] Sanderson K. Bioengineering: What to make with DNA origami. Nature News. 2010;464(7286):158–9.
[46] Sareh P, Chermprayong P, Emmanuelli M, et al. Rotorigami: A rotary origami protective system for robotic rotorcraft. Sci Rob 2018;3(22):h5228.
[47] Sareh P. Symmetric descendents of the Miura-ori. University of Cambridge, 2014.
[48] Sareh P, Guest SD. Minimal isomorphic symmetric variations on the Miura fold pattern. Seville, Spain: 2013.
[49] Sareh P, Guest SD. Design of isomorphic symmetric descendants of the Miura-ori. Smart Mater Struct 2015;24(8):85001.
[50] Sareh P, Guest SD. Design of non-isomorphic symmetric descendants of the Miura-ori. Smart Mater Struct 2015;24(8):85002.
[51] Sareh P, Guest SD. A framework for the symmetric generalisation of the Miura-ori. Int J Space Struct 2015;30(2):141–52.
[52] Sareh P, Guest SD. Tessellating variations on the Miura fold pattern. Seoul, South Korea: 2012.
[53] Sareh P, Guest SD, Designing symmetric derivatives of the Miura-ori. Springer, Cham, 2015: 233–241.
[54] Song Z, Lv C, Liang M, et al. Microscale silicon origami. Small 2016;12(39): 5401–6.
[55] Stachel H, Remarks on Miura-ori, a Japanese folding method. Romania: Technical University of Cluj-Napoca: 2009.
[56] Takeuchi T, Alper JA, Quevedo WC. A simple organ culture method for differentiation of melanocytes in mouse embryonic skin using "origami" membrane filter. 1980, 6(3–4): 101–102.
[57] Tanizawa K. Large displacement configurations of bi-axially compressed infinite plate. Trans Japan Soc Aeronautical Space Sci 1978;20:177–87.
[58] Yasuda H, Miyazawa Y, Charalampidis EG, et al. Origami-based impact mitigation via rarefaction solitary wave creation. Sci Adv 2019;5(5):u2835.
[59] Yasuda H, Yang J. Tunable frequency band structure of origami-based mechanical metamaterials. J Int Assoc Shell Spat Struct 2017;58(4):287–94.
[60] Zhang Z, Ma W, Wu H, et al. A rigid thick Miura-ori structure driven by bistable carbon fibre-reinforced polymer cylindrical shell. Compos Sci Technol 2018;167: 411–20.
[61] Callens SJP, Zadpoor AA. From flat sheets to curved geometries: Origami and kirigami approaches. Mater Today 2018;21(3):241–64.
[62] Qi Z, Campbell DK, Park HS. Atomistic simulations of tension-induced large deformation and stretchability in graphene kirigami. Phys Rev B 2014;90(24): 245437.
[63] Blees MK, Barnard AW, Rose PA, et al. Graphene kirigami. Nature 2015;524 (7564):204–7.
[64] Thiel M, Fischer J, von Freymann G, et al. Direct laser writing of three-dimensional submicron structures using a continuous-wave laser at 532 nm. Appl Phys Lett 2010;97(22):221102.
[65] Ishida M, Fujita J, Ichihashi T, et al. Free-space-wiring fabrication in nano-space by focused-ion-beam chemical vapor deposition. J Vac Sci Technol B Microelectron Nanometer Struct 2003;21(6):2728.
[66] Gansel JK, Thiel M, Rill MS, et al. Gold helix photonic metamaterial as broadband circular polarizer. Science 2009;325(5947):1513–5.
[67] Turner MD, Saba M, Zhang Q, et al. Miniature chiral beamsplitter based on gyroid photonic crystals. Nat Photonics 2013;7(10):801–5.
[68] Liu N, Guo H, Fu L, et al. Three-dimensional photonic metamaterials at optical frequencies. Nat Mater 2008;7(1):31–7.
[69] Barranco A, Borras A, Gonzalez-Elipe AR, et al. Perspectives on oblique angle deposition of thin films: From fundamentals to devices. Prog Mater Sci 2016;76: 59–153.
[70] Chen S, Chen J, Zhang X, et al. Kirigami/origami: unfolding the new regime of advanced 3D microfabrication/nanofabrication with "folding". Light Sci Appl 2020;9(1):s41320–77.
[71] Collins GP. Science and culture: Kirigami and technology cut a fine figure, together. Proc Natl Acad Sci 2016;113(2):240–1.
[72] Park JJ, Won P, Ko SH. A review on hierarchical origami and kirigami structure for engineering applications. Int J Precision Eng Manuf Green Technol 2019;6(1): 147–61.
[73] Liu Z, Cui A, Li J, et al. Folding 2D structures into 3D configurations at the micro/nanoscale: principles, techniques, and applications. Adv Mater 2019;31(4): 1802211.
[74] Liu Z, Du H, Li J, et al. Nano-kirigami with giant optical chirality. Sci Adv 2018;4 (7):t4436.
[75] Grosso BF, Mele EJ. Bending rules in graphene kirigami. Phys Rev Lett 2015;115 (19):195501.
[76] Lv Z, Luo Y, Tang Y, et al. Editable supercapacitors with customizable stretchability based on mechanically strengthened ultralong MnO_2 nanowire composite. Adv Mater 2018;30(2):1704531.
[77] Shyu TC, Damasceno PF, Dodd PM, et al. A kirigami approach to engineering elasticity in nanocomposites through patterned defects. Nat Mater 2015;14(8): 785–9.
[78] Chen Y, Feng J. Folding of a type of deployable origami structures. Int J Struct Stab Dyn 2012;12(6):1250054.
[79] Belcastro S, Hull TC. Modelling the folding of paper into three dimensions using affine transformations. Linear Algebra Appl 2002;348(1):273–82.
[80] Sareh P. The least symmetric crystallographic derivative of the developable double corrugation surface: Computational design using underlying conic and cubic curves. Mater Des 2019;183:108128.
[81] Chen Y, Sareh P, Yan J, et al. An integrated geometric-graph-theoretic approach to representing origami structures and their corresponding truss frameworks. J Mech Design Trans ASME 2019;141(9):091402.
[82] Chen Y, Fan L, Bai Y, et al. Assigning mountain-valley fold lines of flat-foldable origami patterns based on graph theory and mixed-integer linear programming. Comput Struct 2020;239:106328.
[83] Chen Y, Yan J, Feng J, et al. PSO-based metaheuristic design generation of non-trivial flat-foldable origami tessellations with degree-4 vertices. J Mech Des Trans ASME 2021;143(1):011703.
[84] Sareh P, Chen Y. Intrinsic non-flat-foldability of two-tile DDC surfaces composed of glide-reflected irregular quadrilaterals. Int J Mech Sci 2020;185:105881.
[85] Ozaki T, Hosaka H, Morita T. Magnetic flux memory effect using a magnetostrictive material-shape memory piezoelectric actuator composite. Sens Actuat A 2009;154(1):69–72.
[86] Huang W, Li J, Liu D, et al. Polyelectrolyte complex fiber of alginate and poly (diallyldimethylammonium chloride): Humidity-induced shape memory and mechanical transition. ACS Appl Polymer Mater 2020;2(6):2119–25.
[87] Wang E, Wu Y, Islam MZ, et al. A novel reduced graphene oxide/epoxy sandwich structure composite film with thermo-, electro- and light-responsive shape memory effect. Mater Lett 2019;238:54–7.
[88] Chu C, Xiang Z, Wang J, et al. A near-infrared light-triggered shape-memory polymer for long-time fluorescence imaging in deep tissues. J Mater Chem B 2020;8(35):8061–70.
[89] Cho Y, Shin JH, Costa A, et al. Engineering the shape and structure of materials by fractal cut. PNAS 2014;111(49):17390–5.
[90] Tang Y, Yin J. Design of cut unit geometry in hierarchical kirigami-based auxetic metamaterials for high stretchability and compressibility. Extreme Mech Lett 2017;12:77–85.
[91] An N, Domel AG, Zhou J, et al. Programmable hierarchical kirigami. Adv Funct Mater 2019;30(6):1906711.
[92] Jin L, Forte AE, Deng B, et al. Kirigami-inspired inflatables with programmable shapes. Adv Mater 2020;32(33):2001863.
[93] Tang Y, Lin G, Han L, et al. Design of hierarchically cut hinges for highly stretchable and reconfigurable metamaterials with enhanced strength. Adv Mater 2015;27(44):7181–90.
[94] Tang Y, Li Y, Hong Y. Programmable active kirigami metasheets with more freedom of actuation. PNAS 2019;116(52):26407–13.
[95] Babaee S, Pajovic S, Rafsanjani A, et al. Bioinspired kirigami metasurfaces as assistive shoe grips. Nat Biomed Eng 2020;4(8):778–86.
[96] Rafsanjani A, Jin L, Deng B, et al. Propagation of pop ups in kirigami shells. Proc Natl Acad Sci 2019;116(17):8200–5.
[97] Sedal A, Memar AH, Liu T, et al. Design of deployable soft robots through plastic deformation of kirigami structures. IEEE Rob Autom Lett 2020;5(2):2272–9.
[98] Chen SH, Chan KC, Han DX, et al. Programmable super elastic kirigami metallic glasses. Mater Des 2019;169:107687.
[99] Han DX, Zhao L, Chen SH, et al. Critical transitions in the shape morphing of kirigami metallic glass. J Mater Sci Technol 2021;61:204–12.

[100] Taniyama H, Iwase E. Design of rigidity and breaking strain for a kirigami structure with non-uniform deformed regions. Micromachines 2019;10(6): i10060395.
[101] Chen SH, Chan KC, Yue TM, et al. Highly stretchable kirigami metallic glass structures with ultra-small strain energy loss. Scr Mater 2018;142:83–7.
[102] Isobe M, Okumura K. Initial rigid response and softening transition of highly stretchable kirigami sheet materials. Sci Rep 2016;6(1):p24758.
[103] Hwang D, Bartlett MD. Tunable mechanical metamaterials through hybrid kirigami structures. Sci Rep 2018;8(1):s41518–98.
[104] Tang Y, Lin G, Yang S, et al. Programmable kiri-kirigami metamaterials. Adv Mater 2017;29(10):1604262.
[105] Yang Y, Dias MA, Holmes DP. Multistable kirigami for tunable architected materials. Phys Rev Mater 2018;2(11):110601.
[106] Bahamon DA, Qi Z, Park HS, et al. Graphene kirigami as a platform for stretchable and tunable quantum dot arrays. Phys Rev B 2016;93(23):235408.
[107] An N, Li M, Zhou J. Modeling SMA-enabled soft deployable structures for kirigami/origami reflectors. Int J Mech Sci 2020;180:105753.
[108] Zheng W, Huang W, Gao F, et al. Kirigami-inspired highly stretchable nanoscale devices using multidimensional deformation of monolayer MoS_2. Chem Mater 2018;30(17):6063–70.
[109] Zhao Y, Wang C, Wu J, et al. Carbon nanotubes kirigami mechanical metamaterials. PCCP 2017;19:11032–42.
[110] Sadoc JF, Charvolin J, Rivier N. Phyllotaxis on surfaces of constant Gaussian curvature. J Phys A Math Theor 2013;46(29):295202.
[111] Sadoc JF, Rivier N, Charvolin J. Phyllotaxis: a non-conventional crystalline solution to packing efficiency in situations with radial symmetry. Acta Crystallogr A 2012;68(4):470–83.
[112] Castle T, Cho Y, Gong X, et al. Making the cut: lattice kirigami rules. Phys Rev Lett 2014;113(24):245502.
[113] Castle T, Sussman DM, Tanis M, et al. Additive lattice kirigami. Science. Advances 2016;2(9):e1601258.
[114] Sussman DM, Cho Y, Castle T, et al. Algorithmic lattice kirigami: A route to pluripotent materials. Proc Natl Acad Sci 2015;112(24):7449–53.
[115] Mcgregor AD, Mcgregor IA. Fundamental techniques of plastic surgery. London: Churchill Livingstone, 2000.
[116] Chen Y, Sareh P, Feng J, et al. A computational method for automated detection of engineering structures with cyclic symmetries. Comput Struct 2017;191: 153–64.
[117] Chen Y, Feng J, Liu Y. A group-theoretic approach to the mobility and kinematic of symmetric over-constrained structures. Mech Mach Theory 2016;105:91–107.
[118] Lv C, Krishnaraju D, Konjevod G, et al. Origami based mechanical metamaterials. Scientific Reports. 2015, 4(1): p. 5979.
[119] Evans TA, Lang RJ, Magleby SP, et al. Rigidly foldable origami gadgets and tessellations. R Soc Open Sci 2015;2(9):150067.
[120] Eidini M, Paulino GH. Unraveling metamaterial properties in zigzag-base folded sheets. Sci Adv 2015;1(8):e1500224.
[121] Eidini M. Zigzag-base folded sheet cellular mechanical metamaterials. Extreme Mech Lett 2016;6:96–102.
[122] Xia L, Wu W, Xu J, et al. 3D nanohelix fabrication and 3D nanometer assembly by focused ion beam stress-introducing technique. Istanbul, TURKEY: 2006.
[123] Mao Y, Pan Y, Zhang W, et al. Multi-direction-tunable three-dimensional meta-atoms for reversible switching between midwave and long-wave infrared regimes. Nano Lett 2016;16(11):7025–9.
[124] Chalapat K, Chekurov N, Jiang H, et al. Self-organized origami structures via ion-induced plastic strain. Adv Mater 2013;25(1):91–5.
[125] Tang Y, Liu Z, Deng J, et al. Nano-kirigami metasurface with giant nonlinear optical circular dichroism. Laser Photonics Rev 2020;14(7):2000085.
[126] Liu Z, Xu Y, Ji CY, et al. Fano-enhanced circular dichroism in deformable stereo metasurfaces. Adv Mater 2020;32(8):e1907077.
[127] Li J, Liu Z. Focused-ion-beam-based nano-kirigami: From art to photonics. Nanophotonics 2018;7(10):1637–50.
[128] Matsui S, Kaito T, Fujita J, et al. Three-dimensional nanostructure fabrication by focused-ion-beam chemical vapor deposition. J Vac Sci Technol B 2000;18(6): 3181–4.
[129] Utke I, Hoffmann P, Melngailis J. Gas-assisted focused electron beam and ion beam processing and fabrication. J Vac Sci Technol B 2008;26(4):1197–276.
[130] Song Z, Wang X, Lv C, et al. Kirigami-based stretchable lithium-ion batteries. Sci Rep 2015;5(1):p10988.
[131] Lamoureux A, Lee K, Shlian M, et al. Dynamic kirigami structures for integrated solar tracking. Nat Commun 2015;6(1):s9092.
[132] Wu C, Wang X, Lin L, et al. Paper-based triboelectric nanogenerators made of stretchable interlocking kirigami patterns. ACS Nano 2016;10(4):4652–9.
[133] Dijvejin ZA, Kazemi KK, Alasvand Zarasvand K, et al. Kirigami-enabled microwave resonator arrays for wireless, flexible, passive strain sensing. ACS Appl Mater Interf 2020;12(39):44256–64.
[134] Yamamoto Y, Harada S, Yamamoto D, et al. Printed multifunctional flexible device with an integrated motion sensor for health care monitoring. Sci Adv 2016; 2(11):e1601473.
[135] Jang N, Kim K, Ha S, et al. Simple approach to high-performance stretchable heaters based on kirigami patterning of conductive paper for wearable thermotherapy applications. ACS Appl Mater Interf 2016;9(23):19612–21.
[136] Guo Y, Dun C, Xu J, et al. Ultrathin, washable, and large-area graphene papers for personal thermal management. Small. 2017, 13(44): 1702645.